Angewandte Zuschriften

VIP Alloys Very Important Paper

Deutsche Ausgabe: DOI: 10.1002/ange.201501049
Internationale Ausgabe: DOI: 10.1002/anie.201501049

Origin of Extraordinary Stability of Square-Planar Carbon Atoms in Surface Carbides of Cobalt and Nickel**

Anjan Nandula, Quang Thang Trinh, Mark Saeys, and Anastassia N. Alexandrova**

Angewandte Chemie

Abstract: *Surface carbides of cobalt and nickel are exceptionally stable, having stabilities competitive with those of graphitic C on these surfaces. The unusual structure of these carbides has attracted much attention: C assumes a tetracoordinate square-planar arrangement, in-plane with the metal surface, and its binding favors a spontaneous p4g clock surface reconstruction. A chemical bonding model for these systems is presented and explains the unusual structure, special stability, and the reconstruction. C promotes local two-dimensional aromaticity on the surface and the aromatic arrangement is so powerful that the required number of electrons is taken from the void M_4 squares, thus leading to Peierls instability. Moreover, this model predicts a series of new transition-metal and main-group-element surface alloys: carbides, borides, and nitrides, which feature high stability, square-planar coordination, aromaticity, and a predictable degree of surface reconstruction.*

Stable systems containing square-planar (sqpl) carbon atoms are intriguing because tetracoordinate C is typically tetrahedral. Hence, sqpl-C systems have been the focus of many attempts at design and rationalization.[1–23] Current conjectures include the need for electropositive σ-donor/π-acceptor ligands for promoting strong electron delocalization, magic electron counts, aromaticity, and a lack of covalency involving C.[5–21] Most of these efforts are directed toward gas-phase species. Formation of sqpl C on metal surfaces is the least well understood,[4,22,23] yet is of the greatest technological importance, and is the subject of this work.

Sqpl C binds to cobalt and nickel with a remarkable affinity, thus competing with the most stable forms of carbon. It was observed on the Ni(100) surface,[24,25] growing from the step edges on stepped Ni(111) after CO and ethene[22,26] deposition, and, more recently, on Co surfaces (Figure 1).[27–30] These structures are involved in surface corrugation[27,28] and catalyst deactivation.[28,31] Also, the B5 step sites are known to be highly active,[32–35] and a link was made between this high activity and the presence of sqpl C on these sites.[36] The p4g reconstruction of the (100) surface involves a rotation of the two squares in the unit cell, as well as a slight expansion of the metal–metal (M–M) distance. For the p4g reconstructed Co and Ni carbides, the C bonding energies are very high: 743 and 791 kJ mol^{-1}, respectively.

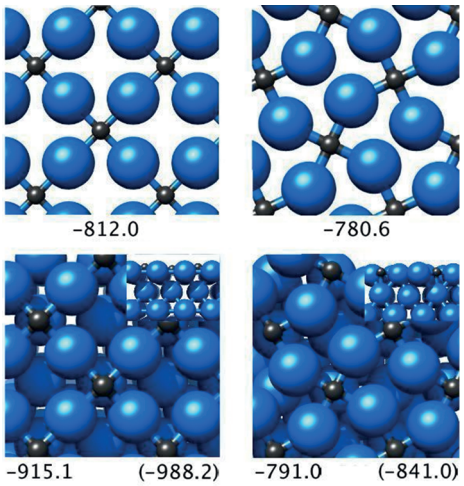

Figure 1. Sqpl C on Co surfaces. a) Non-reconstructed Co(100) monolayer with $^1/_2$ ML C coverage. b) p4g reconstructed Co(100) monolayer with $^1/_2$ ML C coverage. c) Non-reconstructed Co(100) monolayer with $^1/_2$ ML C coverage on the Co(100) fcc slab. d) p4g reconstructed monolayer of Co(100) with $^1/_2$ ML C coverage on a Co(100) fcc slab. The numbers are the calculated C binding energies per C with respect to C in the gas phase and the clean surfaces, in kJ mol^{-1}, calculated with RPBE and (PBE) functionals.

This bonding is stronger than in graphite, graphene islands on Ni and Co surfaces, and diamond.[28,36,37] What governs the formation of such unusual and highly stable structures? Are there any other similar surface alloys?

Arguably, the hallmark gas-phase sqpl-C cluster is Al_4C^{2-} (D_{4h}),[20] thus exhibiting a few apparent similarities with extended surface carbides. Both in Al_4C^{2-} and in p4g surfaces, the symmetry assumes the full suppression of sp hybridization at C.[20,21] The bonding between the metal and the sqpl C is ionic: in Al_4C^{2-} C holds a −2 charge, and in the top layer of Ni/Co carbides it is −1.15/−1.10. This difference is driven by the differences in electronegativities of C and the metal. Through this electronic exercise, the Al_4 square in Al_4C^{2-} has just the proper number of electrons to be stabilized as a result of triple aromaticity.[20,21] What about extended carbides?

The simplest model we considered was the top monolayer of Co_2C with half monolayer ($^1/_2$ ML) coverage of C. Just like the top layer of the slab, the monolayer spontaneously undergoes reconstruction with comparable energy gain and resultant charge distribution. The effect of the slab, underneath the monolayer, on the bonding in is apparently minimal because the C-binding energies to the preformed p4g sites on Co(100) and Co(111) are nearly identical.[28] It appears that the top monolayer of Co_2C exhibits a localization of electron density around C, with diminished overlap between C-containing squares (Figure 2). Hence, a localized bonding model might provide qualitative insight. The d-states, which do not involve contributions from C, are delocalized over the entire lattice.

In the prototypical example of Al_4C^{2-}, σ-radial, σ-peripheral, and π-delocalized bonding are found (Figure 3 A). Similarly, when d atomic orbitals (AOs) are involved in Co_2C, the possible delocalized overlaps include σ-radial, σ-peripheral, π-radial, π-peripheral, and δ (Figure 3 B). Of those, σ-

[*] A. Nandula, Prof. A. N. Alexandrova
Department of Chemistry and Biochemistry
University of California Los Angeles
607 Charles E. Young Drive, Los Angeles, CA 90095-1569 (USA)
E-mail: ana@chem.ucla.edu
Q. T. Trinh
Department of Chemical and Biomolecular Engineering
National University of Singapore
Prof. M. Saeys
Laboratory for Chemical Technology, Gent University
Technologiepark-Zwijnaarde 914, 9052 Gent (Belgium)
E-mail: mark.saeys@ugent.be

[**] Financial support comes from the Alfred P. Sloan Fellowship, the NSF-CAREER Award CHE-1351968 to A.N.A., and the Odysseus Type I grant from the Research Foundation-Flanders to M.S.
Supporting information for this article is available on the WWW under http://dx.doi.org/10.1002/anie.201501049.

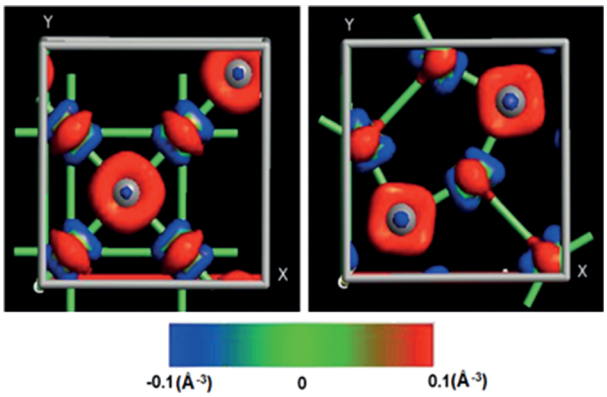

Figure 2. Electron density builds up around C upon binding to non-reconstructed (left) and reconstructed (right) (100) monolayers, shown with respect to the superposition of individual atomic densities: red: density gain, blue: density loss.

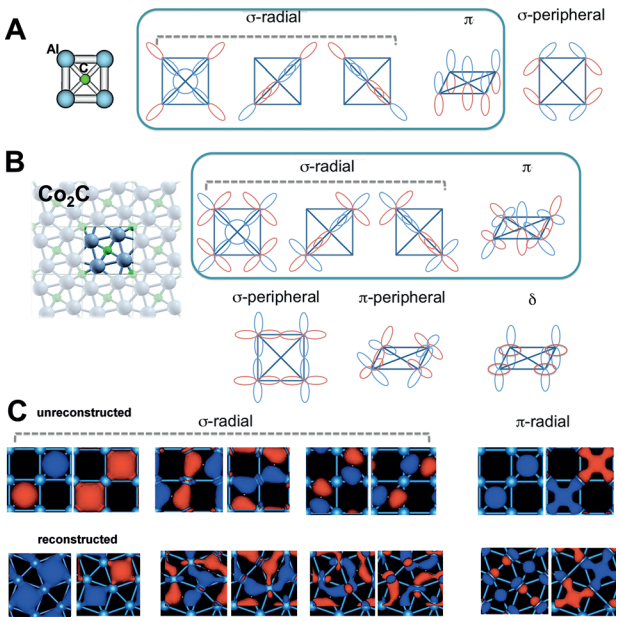

Figure 3. A) Schematic representation of molecular orbitals (MOs) in Al_4C^{2-}. These states make the system triply aromatic.[20,21] B) Schematic representation of Bloch states in the Co_4C unit of the Co_2C monolayer. In both cases, the states that bind C are outlined. C) The states in the non-reconstructed and reconstructed Co_2C monolayer, plotted at the Γ point, corresponding to those outlined in (B). They come in pairs because the unit cell is 2×2.

radial mixes with the 2s and $2p_x$,p_y AOs on C, and π-radial mixes with the $2p_z$ AO on C. The corresponding Bloch states for non-reconstructed and reconstructed surfaces are shown in Figure 3C.

The π-state in Figure 3C could formally be seen as a periodic analogue of π-aromaticity, wherein two electrons are localized over a single square and it obeys Hückel's $(4n+2)$ rule for aromaticity $(n=0)$. The states formed by the 2s and $2p_{x,y}$ AOs on C form three pairs of Bloch states of the σ-radial type. By analogy with the radial overlap in Al_4C^{2-}, these states make the square locally σ-aromatic, with six σ-electrons obeying the $(4n+2)$ rule for the second time $(n=1)$.[20,21] All these bands are located below E_F, thus making the electron count per unit cell straightforward. Therefore, the electron count is akin to the double local aromaticity: σ-radial and π, by Hückel's approximation. In line with the stabilizing effect of aromaticity, surface states supported by the AOs of C undergo a dramatic stabilization compared to the clean (100) surface (see Figure S1 in the Supporting Information). The stabilizing effect of aromaticity, attained through the local electron-deficiency and fully-bonded nature of the states involving sqpl C, is responsible for the unusual stability and high binding energies of C in Co_2C. States that do not involve C exhibit the remaining types of delocalized overlap: σ-peripheral, π-peripheral, and δ (see Figure S2). Furthermore, the aromatic states involving sqpl C appear to be exactly the same for Co_2C, Ni_2C, and, as a matter of fact all optimized surface alloys of the p4g-type formed by every combination of B, C, N and Co, Ni, Cu, Rh, Pd, Ag. (Figure S2). Aromaticity is a strong bonding effect which enforces the proper electron count in all these systems regardless of the composition.

Now why do carbides undergo reconstruction? And why does Co_2C undergo reconstruction more readily than Ni_2C? It appears that the void M_4 squares serve as electron reservoirs, thus either giving or taking electrons to generate the aromaticity of M_4C units. There exist states across the M–M diagonal of all possible types: σ, π, and δ (Figure 4A). The bonding states are filled, but the number of filled antibonding states varies depending on the composition of the system. Electrons removed from these antibonding states effectively increase the M–M bond order, thus turning squares into rhombuses by Peierls instability, thus constituting reconstruction.

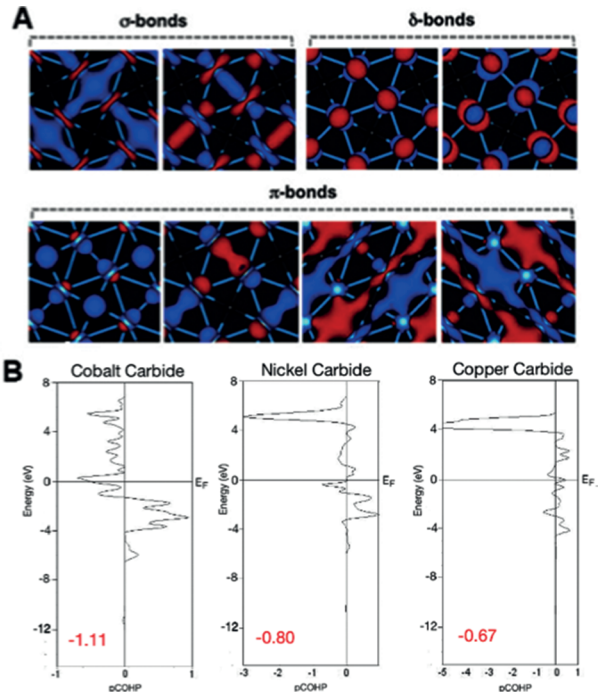

Figure 4. A) Void square M–M bonds after the reconstruction. B) COHP curves of the void square M–M bonds and their definite integrals up to the E_F (in red) for the first row (100) reconstructed carbide monolayers.

To quantify the relative amount of bonding and antibonding in the M–M region of the void square/rhombus, we performed crystal orbital Hamiltonian population (COHP)[40–42] analysis. The integral of the COHP curve in the M–M region up to E_F scales like the M–M bond energy, and an increasing negative definite integral corresponds to enhanced bonding. The COHP curves for the M–M bond in Co, Ni, and Cu carbides are shown in Figure 4B. In accord with our conjecture, the M–M bonding decreases as the number of d electrons in the system grows and antibonding M–M states get filled. Accordingly, the energy gain upon reconstruction goes down (see Table S1).

The relative COHP values for all considered monolayers are given in Table 1 and the energy profiles for the reconstruction of the monolayers in Figure 5 (see also Figures S3 and S4) further illustrate our point. With some outliers to be addressed in the future (such as weak Pd trends), we now see a clear correlation between the overall electron count, M–M bonding, and the depth of the well for the reconstructed system. In the case of Co boride, carbide, nitride, and oxide, (Figure 5A) reconstruction becomes increasingly less favorable as the number of electrons increases. Borides undergo reconstruction more than carbides and nitrides, and oxides do not undergo reconstruction. This trend correlates with the bonding energy across the void square (Table 1). Further, when considering carbides of transition metals with different numbers of d electrons (Co, Ni, Cu, Rh, Pd, and Ag), there is a decrease in the M–M bonding across the diagonal (Table 1) and in the well-depth on the reconstruction profile (Figure 5B), as the number of d electrons increases. Co, Rh, Ni, and Pd are metals which are more likely to form reconstructed alloys. Thus, with some exceptions to the rule (e.g. Pd; Table 1), systems with more electron-rich main-group elements or transition metals have more antibonding M–M states filled in the void square and undergo reconstruction to a lesser extent. Electron-poor systems result in fewer filled antibonding states, stronger M–M bonding, and stronger reconstruction. However, the aromatic states involving bonding with the main-group element remain the same. This data corroborates our conjecture concerning electron count and aromaticity, and its affiliation with the degree of reconstruction.

Table 1: Reconstruction COHP values (in units of eV).

Metal/Dopant	B	C	N	O
Co	−1.366	−1.108	−0.982	−0.892
Ni	−0.769	−0.796	−0.829	0.203
Cu	−1.033	−0.666	−0.609	−0.370
Rh	−1.232	−0.912	−0.882	−0.752
Pd	−0.054	−0.068	−0.067	−0.060
Ag	−0.433	−0.405	−0.357	−0.197

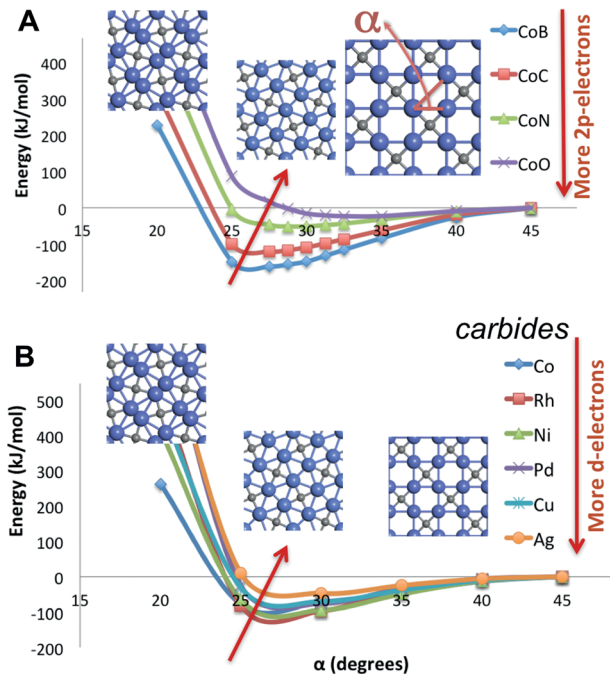

Figure 5. Reconstruction profiles for A) boride, carbide, nitride, and oxide of Co and B) carbides of Co, Ni, Cu, Rh, Pd, Ag. The electron count correlates with the eneergy gain upon reconstruction. As the number of electrons in the system grows, whether coming from the metal or the main-group element, the reconstruction minimum either becomes shallower or disappears.

Extending the discussion from the monolayers to the slabs is straightforward (see Figure S5 and Tables S2 and S3). In general, the surface alloys mimic the monolayers in the structures and well-depths for the reconstruction, except for Rh. Consistent with the findings of the effective medium theory of Norskov et al., binding energies decrease with an increasing d-electron count.[43] However, structures other than flat surface alloys are possible for these materials, so we checked this next. We found that although borides undergo reconstruction,[37,44] many of them undergo significant distortions with B also binding to the subsurface layer. However, depending on the method of preparation, surface borides can be made to promote the Co and Ni catalysts.[44,45] Carbides prefer the (near-)p4g structure: C sits slightly above the plane in d^8 systems and Ni, lies planar in d^{10} systems, and goes subsurface in Pd. Ag_2C is the only surface carbide to not reconstruct. Surface nitrides, with the exception of Pd_2N, do not undergo reconstruction, and the N atom lies subsurface and causes distortions similar to those found in the borides. Oxides do not undergo reconstruction, and the O atom sits above the plane of the surface by approximately an Ångstrøm.

After removing the alloys, which prefer structures other than p4g or p4g slightly deviated from planarity, from the discussion, the following stable, two-dimensional, locally aromatic, and strongly reconstructed surface alloys are predicted: Co_2B, Co_2C, Ni_2B, Ni_2C, Cu_2B, Cu_2C, Pd_2B, Pd_2C, Pd_2N, and Ag_2B. Of these examples the Cu, Pd, and Ag systems have not been reported, although Pd_2B was previously studied and predicted to have different structure from the one found in this work.[46] All of the new alloys may be of a great importance in, for example, catalysis.

Computational Methods

All energies and geometries were calculated with plane-wave PAW DFT and the revised PBE functional[47,48] using VASP.[49–52] The Brillouin zone was sampled with a (5 × 5 × 1) Monkhorst-Pack k-point

grid and plane-waves energies were bounded by a 450 eV cutoff. Monolayers were modelled with 2×2 fcc (100) unit cells, separated with a vacuum gap three times the respective lattice constant. Slabs were modelled with $2\times2\times5$ unit cells, with the monolayer carbide stretched slightly to match the lattice constant underneath. For octahedral geometries, the main group element was displaced accordingly, before optimization. The bottom three layers remained fixed while the top two layers were relaxed. Bloch states were calculated using the Quantum Espresso (QE)[53] package with PBE. COHP curves were generated with Lobster[40,41] and visualized in wxDragon.[54]

Keywords: alloys · aromaticity · bond energy · cobalt · density functional calculations

How to cite: *Angew. Chem. Int. Ed.* **2015**, *54*, 5312–5316
Angew. Chem. **2015**, *127*, 5402–5406

[1] J. Silvestre, R. Hoffman, *Inorg. Chem.* **1985**, *24*, 4108–4119.
[2] R. Hoffmann, R. W. Alder, C. F. Wilcox, Jr., *J. Am. Chem. Soc.* **1970**, *92*, 4992.
[3] R. Hoffmann, *Pure Appl. Chem.* **1971**, *28*, 181.
[4] E. F. Merschrod, S. H. Tang, R. Hoffmann, *Z. Naturforsch.* **1998**, *53b*, 322–332.
[5] J. B. Collins, J. D. Dill, E. D. Jemmis, Y. Apeloig, P. von R. Schleyer, R. Seeger, J. A. Pople, *J. Am. Chem. Soc.* **1976**, *98*, 5419.
[6] R. Keese, *Chem. Rev.* **2006**, *106*, 4787.
[7] G. Merino, M. A. Mendez-Rojas, A. Vela, T. Heine, *J. Comput. Chem.* **2007**, *28*, 362.
[8] W. Siebert, A. Gunale, *Chem. Soc. Rev.* **1999**, *28*, 367.
[9] D. Röttger, G. Erker, *Angew. Chem. Int. Ed. Engl.* **1997**, *36*, 812; *Angew. Chem.* **1997**, *109*, 840.
[10] A. C. Castro, M. Audiffred, J. M. Mercero, J. M. Ugalde, M. A. Mendez-Rojas, G. Merino, *Chem. Phys. Lett.* **2012**, *519*, 29.
[11] K. Exner, P. von R. Schleyer, *Science* **2000**, *290*, 1937.
[12] Z.-X. Wang, P. von R. Schleyer, *J. Am. Chem. Soc.* **2001**, *123*, 994.
[13] Z.-X. Wang, T. K. Manojkumar, C. Wannere, P. von R. Schleyer, *Org. Lett.* **2001**, *3*, 1249.
[14] Z.-X. Wang, P. von R. Schleyer, *Science* **2001**, *292*, 2465.
[15] Z. X. Wang, P. von R. Schleyer, *J. Am. Chem. Soc.* **2002**, *124*, 11979.
[16] C. S. Wannere, C. Corminboeuf, Z.-X. Wang, M. D. Wodrich, R. B. King, P. von R. Schleyer, *J. Am. Chem. Soc.* **2005**, *127*, 5701.
[17] D. Roy, C. Corminboeuf, C. S. Wannere, R. B. King, P. von R. Schleyer, *Inorg. Chem.* **2006**, *45*, 8902.
[18] A. I. Boldyrev, P. von R. Schleyer, *J. Chem. Soc. Chem. Commun.* **1991**, 1536.
[19] Z.-H. Cui, M. Contreras, Y.-H. Ding, G. Merino, *J. Am. Chem. Soc.* **2011**, *133*, 13228.
[20] A. I. Boldyrev, X. Li, L.-S. Wang, *Angew. Chem. Int. Ed.* **2000**, *39*, 3307; *Angew. Chem.* **2000**, *112*, 3445.
[21] A. N. Alexandrova, M. J. Nayhaouse, M. T. Huynh, J. L. Kuo, A. V. Melkonian, G. De J. Chavez, N. M. Hernando, M. D. Kowal, *Phys. Chem. Chem. Phys.* **2012**, *14*, 14815–14821.
[22] C. Klink, I. Stensgaard, F. Besenbacher, E. Lægsgaard, *Surf. Sci.* **1995**, *342*, 250–260.
[23] S. Stolbov, S. Hong, K. Abdelkader, T. S. Rahman, *Phys. Rev. B* **2005**, *72*, 155423.
[24] J. H. Onuferko, D. P. Woodruff, B. W. Holland, *Surf. Sci.* **1979**, *87*, 357–374.
[25] K. H. Rieder, H. Wilsch, *Surf. Sci.* **1983**, *131*, 245–257.
[26] R. T. Vang, K. Honkala, S. Dahl, E. K. Vestergaard, J. Schnadt, E. Lægsgaard, B. S. Clausen, J. K. Nørskov, F. Besenbacher, *Surf. Sci.* **2006**, *600*, 66–77.
[27] I. M. Ciobîcă, R. A. van Santen, P. J. van Berge, J. van de Loosdrecht, *Surf. Sci.* **2008**, *602*, 17–27.
[28] K. F. Tan, J. Xu, J. Chang, A. Borgna, M. Saeys, *J. Catal.* **2010**, *274*, 121–129.
[29] Q. T. Trinh, K. F. Tan, A. Borgna, M. Saeys, *J. Phys. Chem. C* **2013**, *117*, 1684–1691.
[30] C. J. Weststrate, A. C. Kızılkaya, E. T. R. Rossen, M. W. G. M. Verhoeven, I. M. Ciobîcă, A. M. Saib, J. W. (Hans) Niemantsverdriet, *J. Phys. Chem. C* **2012**, *116*, 11575–11583.
[31] A. M. Saib, D. J. Moodley, I. M. Ciobîcă, M. M. Hauman, B. H. Sigwebela, C. J. Weststrate, J. W. Niemantsverdriet, J. van de Loosdrecht, *Catal. Today* **2010**, *154*, 271–282.
[32] R. van Hardeveld, A. van Montfoort, *Surf. Sci.* **1966**, *4*, 396–430.
[33] R. van Hardeveld, F. Hartog, *Surf. Sci.* **1969**, *15*, 189–230.
[34] R. A. Van Santen, *Acc. Chem. Res.* **2009**, *42*, 57–66.
[35] R. T. Vang, K. Honkala, S. Dahl, E. K. Vestergaard, J. Schnadt, E. Lægsgaard, B. S. Clausen, J. K. Nørskov, F. Besenbache, *Nat. Mater.* **2005**, *4*, 160–162.
[36] A. Banerjee, A. P. van Bavel, H. P. C. E. Kuipers, M. Saeys, unpublished results.
[37] J. Xu, M. Saeys, *J. Phys. Chem. C* **2009**, *113*, 4099–4106.
[38] J. Chandrasekhar, E. D. Jemmis, P. von R. Schleyer, *Tetrahedron Lett.* **1979**, *39*, 3707–3710.
[39] J. Wilson, C. de Groot, *J. Phys. Chem. B* **1995**, *99*, 7860.
[40] R. Dronskowski, P. E. Blöchl, *J. Phys. Chem.* **1993**, *97*, 8617–8624.
[41] V. L. Deringer, A. L. Tchougreeff, R. Dronskowski, *J. Phys. Chem. A* **2011**, *115*, 5461–5466.
[42] S. Maintz, V. L. Deringer, A. L. Tchougreeff, R. Dronskowski, *J. Comput. Chem.* **2013**, *34*, 2557–2567.
[43] J. K. Nørskov, N. D. Lang, *Phys. Rev. B* **1980**, *21*, 2131–2136.
[44] J. Xu, L. Chen, K. F. Tan, A. Borgna, M. Saeys, *J. Catal.* **2009**, *261*, 158.
[45] K. F. Tan, J. Chang, A. Borgna, M. Saeys, *J. Catal.* **2011**, *280*, 50.
[46] C. W. A. Chan, A. H. Mahadi, M. M.-J. Li, E. C. Corbos, C. Tang, G. Jones, W. C. H. Kuo, J. Cookson, C. M. Brown, P. T. Bishop, S. C. E. Tsang, *Nat. Commun.* **2014**, *5*, 5787.
[47] J. P. Perdew, K. Burke, M. Ernzerhof, *Phys. Rev. Lett.* **1996**, *77*, 3865.
[48] J. P. Perdew, K. Burke, M. Ernzerhof, *Phys. Rev. Lett.* **1997**, *78*, 1396.
[49] G. Kresse, J. Hafner, *Phys. Rev. B* **1993**, *47*, 558.
[50] G. Kresse, J. Hafner, *Phys. Rev. B* **1994**, *49*, 14251.
[51] G. Kresse, J. Furthmüller, *Compt. Mater. Sci.* **1996**, *6*, 15.
[52] G. Kresse, J. Furthmüller, *Phys. Rev. B* **1996**, *54*, 11169.
[53] P. Giannozzi, S. Baroni, N. Bonini, M. Calandra, R. Car, C. Cavazzoni, D. Ceresoli, G. L. Chiarotti, M. Cococcioni, I. Dabo, A. Dal Corso, S. Fabris, G. Fratesi, S. de Gironcoli, R. Gebauer, U. Gerstmann, C. Gougoussis, A. Kokalj, M. Lazzeri, L. Martin-Samos, N. Marzari, F. Mauri, R. Mazzarello, S. Paolini, A. Pasquarello, L. Paulatto, C. Sbraccia, S. Scandolo, G. Sclauzero, A. P. Seitsonen, A. Smogunov, P. Umari, R. M. Wentzcovitch, *J. Phys. Condens. Matter* **2009**, *21*, 395502.
[54] B. Eck, wxDragon, Aachen, Germany, **1994–2013**; available at http://www.wxdragon.de.

Received: February 3, 2015
Published online: March 24, 2015

